NUMERICAL INVESTIGATION OF THERMOCONCENTRATIONAL CONVECTION IN THE LIQUID CORE OF A CRYSTALLIZING BINARY MELT

P. F. Zavgorodnii

UDC 621.746.7.001

Thermoconcentrational convection in a solidifying binary melt is numerically investigated.

A crystallizing binary melt is characterized not only by temperature inhomogeneity of the liquid core due to the interaction between the thermal motion and the gravitational field, but also, because the impurity is of different solubilities in the solid and liquid phases, by concentration inhomogeneity, which leads to the appearance and development of convective motion – called concentrational convective motion.

The combined interaction with the gravitational field of the temperature and concentration inhomogeneities in the liquid core of a crystallizing binary melt causes thermoconcentrational convective motion in the melt. Nevertheless, several hydrodynamic investigations of the liquid core of a crystallizing melt (see, for example, [1-3]) have considered a pure melt or ignored the effect of the concentration inhomogeneity [4].

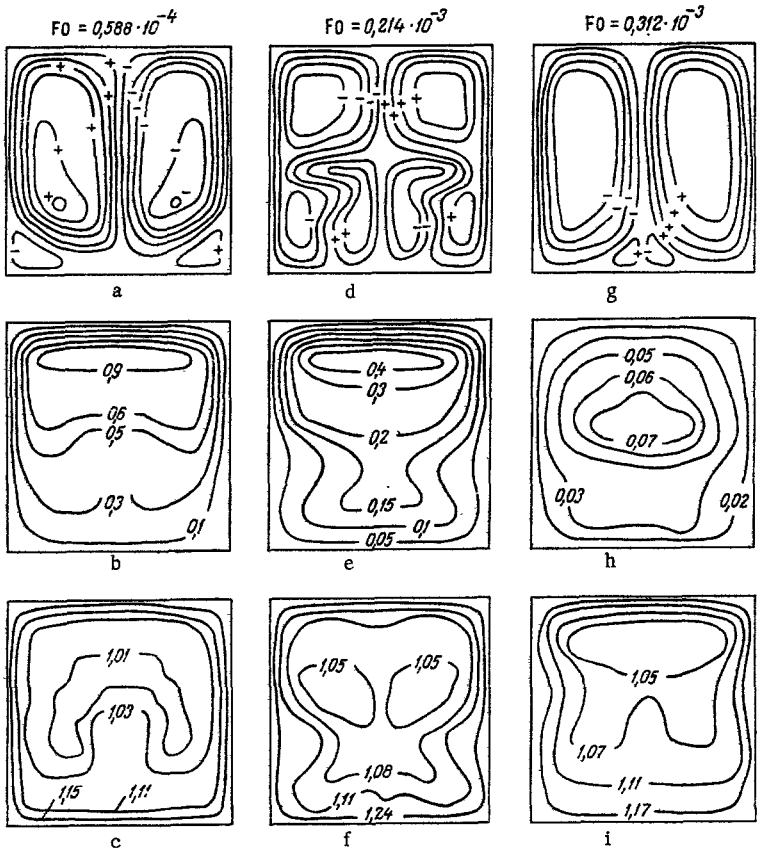

Fig. 1. Change with time of stream isolines (a, d, g), isotherms (b, e, h), and concentration isolines (c, f, i).

Donetsk State University. Translated from Inzhenerno-Fizicheskii Zhurnal, Vol. 35, No. 1, pp. 155-162, July, 1978. Original article submitted February 21, 1977.

0022-0841/78/3501-0870$07.50

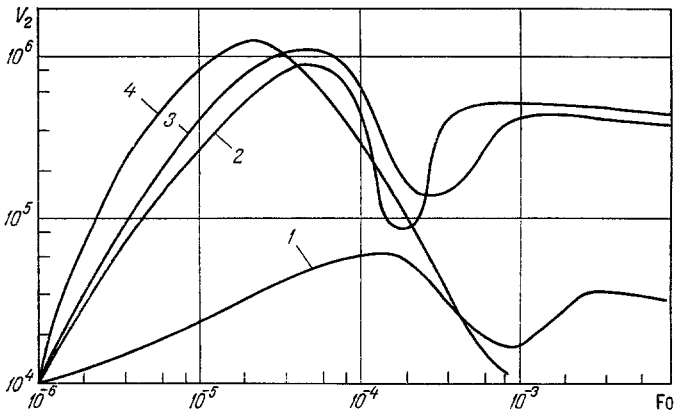

Fig. 2. Change over time in the maximum velocity of a descending convective flow: 1) $Gr = Gr_D = 0.2 \cdot 10^6$; 2) $Gr = 0.2 \cdot 10^7$, $Gr_D = 0.2 \cdot 10^8$; 3) $Gr = Gr_D = 0.2 \cdot 10^7$; 4) $Gr = 0.2 \cdot 10^7$.

Since most substances in a molten state contain a certain amount of impurity, a numerical investigation of the hydrodynamics in the liquid core of a crystallizing binary melt, taking into account both the temperature and concentration inhomogeneity, should serve to bring the theoretical model closer to the actual process and, correspondingly, to give a broader understanding of this process.

The region considered in constructing a mathematical model of the appearance and development of thermoconcentrational convective motion in the liquid core of a crystallizing binary melt is rectangular and semi-infinite along the horizontal axis, with a cross section of relative dimensions $l_1 \times l_2$.

Initially, the melt is in a quiescent state, with a homogeneous initial temperature distribution, $T_0 > T_c$, and a uniform impurity distribution with initial concentration c_0.

Some time later ($t > 0$), the temperature at the boundary of the region decreases discontinuously to the crystallization temperature T_c, and a solid phase forms at the boundary. The moving phase boundary is assumed to be a plane directly separating the solid and liquid regions.

The time dependence of the solid-phase and liquid-core thicknesses is derived from the classical Neumann solution of the Stefan problem. In dimensionless form, the appropriate expressions are as follows:

$$R_i = \alpha \sqrt{\mathrm{Fo}}, \quad \varepsilon_i = l_i - \alpha \sqrt{\mathrm{Fo}} \quad (i = 1, 2),$$

and the corresponding ranges of the variables η_1 and η_2 are

$$R_1 \leqslant \eta_1 \leqslant \varepsilon_1, \quad R_2 \leqslant \eta_2 \leqslant \varepsilon_2.$$

This choice is reasonable. It follows from [3] that taking into account the influence of convective motion in the liquid core on the heat transfer through the solid phase – which is essentially what determined the position of the phase boundary over time – does not have sufficient effect on the final result to justify a more complicated program and a corresponding increase in the computation time.

In dimensionless form, the initial system of equations is as follows: the equation of motion in the Boussinesq approximation, under the condition that the characteristic velocity and pressure are determined by the conditions

$$u_0 = \frac{D}{x_0}, \quad P_{\max} - P_{\min} = \rho \frac{D^2}{x_0^2},$$

$$\frac{\partial \bar{U}}{\partial \mathrm{Fo}} + (\bar{U} \nabla) \bar{U} = -\nabla \pi + \mathrm{Sm} \Delta \bar{U} + \bar{e}_2 \mathrm{Sm}\, \mathrm{Gr}\, \Theta + \bar{e}_2 \mathrm{Sm}^2 \mathrm{Gr}_D S, \tag{1}$$

the heat-transfer equation

$$\frac{\partial \Theta}{\partial \mathrm{Fo}} + (\bar{U} \nabla) \Theta = \frac{1}{\mathrm{Le}} \Delta \Theta, \tag{2}$$

the mass-transfer equation

$$\frac{\partial S}{\partial \mathrm{Fo}} + (\bar{U}\nabla)S = \Delta S, \tag{3}$$

and the continuity equation

$$\nabla \bar{U} = 0. \tag{4}$$

The system (1)-(4) is closed by the boundary conditions

$$\begin{aligned}
&\mathrm{Fo} = 0 \quad \bar{U} = 0, \quad \Theta = 1, \quad S = 1,\\
&\eta_1 = R_1 \quad \frac{\partial S}{\partial \eta_1} = -R_1'(1-k)S,\\
&\eta_1 = \varepsilon_1 \quad \frac{\partial S}{\partial \eta_1} = -\varepsilon_1'(1-k)S,\\
&\eta_2 = R_2 \quad \frac{\partial S}{\partial \eta_2} = -R_2'(1-k)S,\\
&\eta_2 = \varepsilon_2 \quad \frac{\partial S}{\partial \eta_2} = -\varepsilon_2'(1-k)S.
\end{aligned} \tag{5}$$

Introducing the stream function ψ, related to the velocity components u_1 and u_2 by the expressions $u_1 = \frac{\partial \psi}{\partial \eta_2}$, $u_2 = -\frac{\partial \psi}{\partial \eta_1}$, the vorticity $\varphi = \mathrm{rot}\,\bar{U}$, and the new variables $\zeta_1 = \frac{\eta_1 - R_1}{\varepsilon_1 - R_1}$, $\zeta_2 = \frac{\eta_2 - R_2}{\varepsilon_2 - R_2}$, by means of which the cavity is converted from rectangular to square cross section, so that $0 \le \zeta_1 \le 1$ and $0 \le \zeta_2 \le 1$ throughout the whole of the crystallization period, the initial system (1)-(4) and the boundary conditions (5) may be written in the form

$$\begin{aligned}
&\frac{\partial \varphi}{\partial \mathrm{Fo}} + \frac{1}{\varepsilon_1 - R_1}\left\{\frac{1}{\varepsilon_2 - R_2}\frac{\partial \psi}{\partial \zeta_2} - \zeta_1(\varepsilon_1' - R_1') - R_1'\right\}\frac{\partial \varphi}{\partial \zeta_1} -\\
&-\frac{1}{\varepsilon_2 - R_2}\left\{\frac{1}{\varepsilon_1 - R_1}\frac{\partial \psi}{\partial \zeta_1} + \zeta_2(\varepsilon_2' - R_2') + R_2'\right\}\frac{\partial \varphi}{\partial \zeta_2} =\\
&= \mathrm{Sm}\,\Delta_1\varphi - \frac{\mathrm{Sm}^2\mathrm{Gr}}{\varepsilon_1 - R_1}\frac{\partial \Theta}{\partial \zeta_1} + \frac{\mathrm{Sm}^2\mathrm{Gr}_D}{\varepsilon_1 - R_1}\frac{\partial S}{\partial \zeta_1},
\end{aligned} \tag{6}$$

$$\begin{aligned}
&\frac{\partial \Theta}{\partial \mathrm{Fo}} + \frac{1}{\varepsilon_1 - R_1}\left\{\frac{1}{\varepsilon_2 - R_2}\frac{\partial \psi}{\partial \zeta_2} - \zeta_1(\varepsilon_1' - R_1') - R_1'\right\}\frac{\partial \varphi}{\partial \zeta_1} -\\
&-\frac{1}{\varepsilon_2 - R_2}\left\{\frac{1}{\varepsilon_1 - R_1}\frac{\partial \psi}{\partial \zeta_1} + \zeta_2(\varepsilon_2' - R_2') + R_2'\right\}\frac{\partial \Theta}{\partial \zeta_2} = \frac{1}{\mathrm{Le}}\Delta_1\Theta,
\end{aligned} \tag{7}$$

$$\begin{aligned}
&\frac{\partial S}{\partial \mathrm{Fo}} + \frac{1}{\varepsilon_1 - R_1}\left\{\frac{1}{\varepsilon_2 - R_2}\frac{\partial \psi}{\partial \zeta_2} - \zeta_2(\varepsilon_1' - R_1') - R_1'\right\}\frac{\partial S}{\partial \zeta_1} -\\
&-\frac{1}{\varepsilon_2 - R_2}\left\{\frac{1}{\varepsilon_1 - R_1}\frac{\partial \psi}{\partial \zeta_1} + \zeta_2(\varepsilon_2' - R_2') + R_2'\right\}\frac{\partial S}{\partial \zeta_2} = \Delta_1 S,
\end{aligned} \tag{8}$$

$$\varphi = -\Delta_1\psi, \tag{9}$$

$$\begin{aligned}
&\mathrm{Fo} = 0 \quad \bar{U} = 0, \quad \Theta = 1, \quad S = 1,\\
&\zeta_1 = 0, \ \zeta_1 = 1, \ \zeta_2 = 0, \ \zeta_2 = 1 \quad \Theta = 0, \ \frac{\partial \psi}{\partial \zeta_1} = \frac{\partial \psi}{\partial \zeta_2} = 0,\\
&\zeta_1 = 0 \quad \frac{\partial S}{\partial \zeta_1} = -R_1'(\varepsilon_1 - R_1)(1-k)S,\\
&\zeta_1 = 1 \quad \frac{\partial S}{\partial \zeta_1} = -\varepsilon_1'(\varepsilon_1 - R_1)(1-k)S,\\
&\zeta_2 = 0 \quad \frac{\partial S}{\partial \zeta_2} = -R_2'(\varepsilon_2 - R_2)(1-k)S,\\
&\zeta_2 = 1 \quad \frac{\partial S}{\partial \zeta_2} = -\varepsilon_2'(\varepsilon_2 - R_2)(1-k)S.
\end{aligned} \tag{10}$$

Here

$$\Delta_1 = \frac{1}{(\varepsilon_1 - R_1)^2}\frac{\partial^2}{\partial \zeta_1^2} + \frac{1}{(\varepsilon_2 - R_2)^2}\frac{\partial^2}{\partial \zeta_2^2}.$$

Numerical realization of this problem is by means of an implicit finite-difference scheme of variable directions (a longitudinal–transverse scheme) [5]. Uniform coordinate (ω_h) and time (Fo_h) grids are introduced. The same numbers of divisions over the coordinates ζ_1 and ζ_2 (I – M) are chosen, and thus we obtain

$$\omega_h = \left\{\zeta_1 = ih;\ \zeta_2 = mh;\ h = \frac{1}{I} = \frac{1}{M};\ i = 0,\ 1,\ 2,\ \ldots,\ I;\ m = 0,\ 1,\ 2,\ \ldots,\ M\right\};$$

$$\mathrm{Fo}_h = \left\{\mathrm{Fo} = \sum_n n\tau_i;\ \tau_i = \frac{Ah^2}{4};\ 0<A<1;\ n = 1,\ 2,\ 3\ldots\right\}.$$

Using the method of fractional time steps with simultaneous division over the coordinates ζ_1 and ζ_2 [6], Eqs. (6)-(8) are brought to the form

$$\frac{\varphi^{\wedge}_{i,m} - \varphi^{-}_{i,m}}{0{,}5\tau} + \frac{1}{\varepsilon_1 - R_1}\left\{\frac{1}{\varepsilon_2 - R_2}\left(\frac{\partial\psi}{\partial\zeta_2}\right)^{-}_{i,m} - \right.$$
$$\left. - \zeta_1(\varepsilon_1' - R_1') - R_1'\right\}\left(\frac{\partial\varphi}{\partial\zeta_1}\right)^{\wedge}_{i,m} = \frac{\mathrm{Sm}}{(\varepsilon_1 - R_1)^2}\left(\frac{\partial^2\varphi}{\partial\zeta_1^2}\right)^{\wedge}_{i,m} -$$
$$- \frac{\mathrm{Sm}^2\mathrm{Gr}}{\varepsilon_1 - R_1}\left(\frac{\partial\Theta}{\partial\zeta_1}\right)^{-}_{i,m} + \frac{\mathrm{Sm}^2\mathrm{Gr}_D}{\varepsilon_1 - R_1}\left(\frac{\partial S}{\partial\zeta_1}\right)^{-}_{i,m}, \tag{11}$$

$$\frac{\varphi^{+}_{i,m} - \varphi^{\wedge}_{i,m}}{0{,}5\tau} + \frac{1}{\varepsilon_2 - R_2}\left\{\frac{1}{\varepsilon_1 - R_1}\left(\frac{\partial\psi}{\partial\zeta_1}\right)^{-}_{i,m} + \right.$$
$$\left. + \zeta_2(\varepsilon_2' - R_2') + R_2'\right\}\left(\frac{\partial\varphi}{\partial\zeta_1}\right)^{+}_{i,m} = \frac{\mathrm{Sm}}{(\varepsilon_2 - R_2)^2}\left(\frac{\partial^2\varphi}{\partial\zeta_2^2}\right)^{+}_{i,m}, \tag{12}$$

$$\frac{\Theta^{\wedge}_{i,m} - \Theta^{-}_{i,m}}{0{,}5\tau} + \frac{1}{\varepsilon_1 - R_1}\left\{\frac{1}{\varepsilon_2 - R_2}\left(\frac{\partial\psi}{\partial\zeta_2}\right)^{+}_{i,m} - \right.$$
$$\left. - \zeta_1(\varepsilon_1' - R_1') - R_1'\right\}\left(\frac{\partial\Theta}{\partial\zeta_1}\right)^{\wedge}_{i,m} = \frac{1}{\mathrm{Le}\,(\varepsilon_1 - R_1)^2}\left(\frac{\partial^2\Theta}{\partial\zeta_1^2}\right)^{\wedge}_{i,m}, \tag{13}$$

$$\frac{\Theta^{+}_{i,m} - \Theta^{\wedge}_{i,m}}{0{,}5\tau} - \frac{1}{\varepsilon_2 - R_2}\left\{\frac{1}{\varepsilon_1 - R_1}\left(\frac{\partial\psi}{\partial\zeta_1}\right)^{+}_{i,m} + \right.$$
$$\left. + \zeta_2(\varepsilon_2' - R_2') + R_2'\right\}\left(\frac{\partial\Theta}{\partial\zeta_2}\right)^{+}_{i,m} = \frac{1}{\mathrm{Le}\,(\varepsilon_2 - R_2)^2}\left(\frac{\partial^2\Theta}{\partial\zeta_2^2}\right)^{+}_{i,m}, \tag{14}$$

$$\frac{S^{\wedge}_{i,m} - S^{-}_{i,m}}{0{,}5\tau} + \frac{1}{\varepsilon_1 - R_1}\left\{\frac{1}{\varepsilon_2 - R_2}\left(\frac{\partial\psi}{\partial\zeta_1}\right)^{+}_{i,m} - \right.$$
$$\left. - \zeta_1(\varepsilon_1' - R_1') - R_1'\right\}\left(\frac{\partial S}{\partial\zeta_1}\right)^{\wedge}_{i,m} = \frac{1}{(\varepsilon_1 - R_1)^2}\left(\frac{\partial^2 S}{\partial\zeta_1^2}\right)^{\wedge}_{i,m}, \tag{15}$$

$$\frac{S^{+}_{i,m} - S^{\wedge}_{i,m}}{0{,}5\tau} - \frac{1}{\varepsilon_2 - R_2}\left\{\left(\frac{\partial\psi}{\partial\zeta_1}\right)^{+}_{i,m} + \zeta_2(\varepsilon_2' - R_2') + R_2'\right\}\left(\frac{\partial S}{\partial\zeta_2}\right)^{+}_{i,m} = \frac{1}{(\varepsilon_2 - R_2)^2}\left(\frac{\partial^2 S}{\partial\zeta_2^2}\right)^{+}_{i,m}. \tag{16}$$

The superscripts +, Λ, and – in Eqs. (11)-(16) correspond to the (n+1)-th, (n+1/2)-th, and n-th time step.

The Poisson equation – Eq. (9) – may be written in a form suitable for integration as follows:

$$\psi^{s+1}_{i,m} = \psi^{s}_{i,m} + \omega_0\left\{\frac{1}{2\left[(\varepsilon_1 - R_1)^2 + (\varepsilon_2 - R_2)^2\right]}\left[(\varepsilon_2 - R_2)^2(\psi^{s+1}_{i-1,m} + \psi^{s}_{i+1,m}) + \right.\right.$$
$$\left.\left. + (\varepsilon_1 - R_1)^2(\psi^{s+1}_{i,m-1} + \psi^{s}_{i,m+1}) + (\varepsilon_1 - R_1)^2(\varepsilon_2 - R_2)^2 h^2\varphi_{i,m}\right] - \psi^{s}_{i,m}\right\}.$$

Here s is the number of the iteration and ω_0 is the relaxation parameter.

The difference analog of the system of boundary conditions (10) is of the form

$$\psi^{0}_{i,m} = \varphi^{0}_{i,m} = 0,\ \Theta^{0}_{i,m} = 1,\ S^{0}_{i,m} = 1,\ \psi_{0,m} = \psi_{1,m} = \psi_{i,0} = \psi_{i,1} = 0, \tag{17}$$

$$\varphi_{i,0} = -\frac{2}{h^2}\psi_{i,1},\quad \varphi_{i,m} = -\frac{2}{h^2}\psi_{i,M-1},$$
$$\varphi_{0,m} = -\frac{2}{h^2}\psi_{1,m},\quad \varphi_{I,m} = -\frac{2}{h^2}\psi_{I-1,m}, \tag{18}$$

$$S^{\wedge}_{0,m} = \frac{S^{\wedge}_{1,m} + \frac{h^2}{2\cdot 0{,}5\tau} S^{-}_{0,m}}{1 - hR'_1(1-k) + \frac{h^2}{2}\left\{\frac{1}{0{,}5\tau} + R'^{2}_1(1-k)\right\}},$$

$$S^{\wedge}_{I,m} = \frac{S^{\wedge}_{I-1,m} + \frac{h^2}{2\cdot 0{,}5\tau} S^{-}_{I,m}}{1 + h\varepsilon'_1(1-k) + \frac{h^2}{2}\left\{\frac{1}{0{,}5\tau} + \varepsilon'^{2}_1(1-k)\right\}},$$

$$S^{+}_{i,0} = \frac{S^{+}_{i,1} + \frac{h^2}{2\cdot 0{,}5\tau} S^{\wedge}_{i,M}}{1 + hR'_2(1-k) + \frac{h^2}{2}\left\{\frac{1}{0{,}5\tau} + R'^{2}_2(1-k)\right\}}, \qquad (19)$$

$$S^{+}_{i,M} = \frac{S^{+}_{i,M-1} + \frac{h^2}{2\cdot 0{,}5\tau} S^{\wedge}_{i,M}}{1 + h\varepsilon'_2(1-k) + \frac{h^2}{2}\left\{\frac{1}{0{,}5\tau} + \varepsilon'^{2}_2(1-k)\right\}},$$

$$\Theta_{0,m} = \Theta_{I,m} = \Theta_{i,0} = \Theta_{i,M} = 0. \qquad (20)$$

The boundary conditions (18) and (19) were obtained by expansion in Taylor series in the vicinity of the corresponding boundaries, using the initial equations after division over the coordinates and the corresponding conditions from (10).

Using the integrointerpolational method formulated in [5], and determining the auxiliary coefficients in accordance with [5], the system of equations and boundary conditions (11)-(20) may be reduced to a system of algebraic equations, which have been tested on a Dnepr-21 computer.

A numerical investigation was made for the thermal and diffusional Grashof numbers ($Gr = Gr_D = 0.2 \cdot 10^6$, $Gr = Gr_D = 0.2 \cdot 10^7$, $Gr = 0.2 \cdot 10^7$, $Gr_D = 0.2 \cdot 10^8$) for steel with 1% carbon ($c_0 = 1\%$) in the initial overheating of the melt, $\Delta T = T_0 - T_c = 1°C$, with $k = 0.5$.

Trial calculations showed that to satisfy the conditions of mathematical stability and sufficient accuracy of the calculations, a spatial 32×32 grid is necessary.

Analysis of the curves for the case $Gr = Gr_D = 0.2 \cdot 10^7$ (Fig. 1) indicates that some time after the beginning of the process (in this case $Fo = 0.2 \cdot 10^{-3}$), the direction of the convective motion in the liquid core is reversed.

The explanation is evidently as follows. In the given binary melt, the specific weight of the impurity (carbon) is less than that of the basic melt (iron). Therefore, the convective motion produced by the concentration inhomogeneity which arises in the course of the process is in the opposite direction to the thermal convection due to the temperature inhomogeneity. However, at times shortly after the beginning of the process, the temperature inhomogeneity develops considerably more rapidly than the concentration inhomogeneity (Fig. 1b, c), so that at this time it is the thermal convective motion which determines the overall direction of the motion in the liquid core (Fig. 1a).

As the initial temperature excess of the liquid core is removed (estimates show that this temperature excess persists for 15-20% of the total time of crystallization), the temperature inhomogeneity equalizes (Fig. 1e). Against this background, the effect on the melt of the concentration inhomogeneity, which has become sufficiently well developed by this time, begins to be more clearly expressed (Fig. 1d, f).

From the time that the temperature inhomogeneity is practically equalized (Fig. 1h) and the concentration inhomogeneity, being more stable, is sufficiently well developed (Fig. 1i), the direction of convective motion in the liquid core is completely determined by the concentrational convective motion, which is in the opposite direction to the thermal convection (Fig. 1g).

For the cases $Gr = Gr_D = 0.2 \cdot 10^6$ and $Gr = 0.2 \cdot 10^7$, $Gr_D = 0.2 \cdot 10^8$, the thermoconcentrational convective motion remains basically the same as for the case $Gr = Gr_D = 0.2 \cdot 10^8$, although the rate of development of the process over time and the velocity of the motion are different (Fig. 2). Thus, comparison of curves 1 and 2 shows that if the thermal and diffusional Grashof numbers are equal ($Gr = Gr_D$) the rate of development of the process is higher and the velocity of convective motion in the liquid core is greater in cases of larger Grashof numbers. Comparison of curves 2 and 3 indicates that for equal Grashof numbers, the thermal intensity of the development of the process is less and the velocity of convective motion in the liquid core up to the time that

concentrational convective motion becomes dominant is smaller in cases with larger diffusional Grashof numbers. However, in these cases the reversal in the direction of convective motion in the liquid core occurs more rapidly.

The explanation is evidently that a larger diffusional Grashof number corresponds to more developed concentration inhomogeneity of the liquid core. As a result, the concentration inhomogeneity begins to predominate more quickly over the temperature inhomogeneity, and hence the time in which the concentrational convection comes to determine the overall direction of convective motion in the liquid core is reduced.

Comparison of curves 1-3 with curve 4 [4] indicates that thermoconcentrational convection, unlike thermal convection, occurs in the liquid core of a crystallizing melt practically up to the end of solidification.

NOTATION

x_0, characteristic dimension; c, c_0, current and initial impurity concentration; ρ, density of melt; ν, kinematic viscosity; P, current pressure in liquid core; e_2, unit vector in the direction of the acceleration of gravity; β, thermal-expansion coefficient; γ, diffusional-expansion coefficient; $\bar{g}$, acceleration of gravity; T, current temperature of liquid core; a, thermal diffusivity; k, equilibrium-distribution coefficient; r_i, e_i ($i = 1, 2$), coordinates of phase boundary in the coordinate system; α, solidification coefficient; D, diffusion coefficient; $\bar{u}$, velocity of convective motion in liquid core; L_1, L_2, height and width of crystallizer plane; $\eta_i = x_i/x_0$, dimensionless coordinates; $l_1 = L_1/x_0$, $l_2 = L_2/x_0$, height and width of cavity in the coordinate system $0\eta_1\eta_2$; $R_i = r_i/x_0$, $\varepsilon_i = l_i/x_0$, coordinates of phase boundary in the coordinate system $0\eta_1\eta_2$; $\bar{U} = \bar{u}/u_0$, dimensionless velocity of convective motion in the liquid core; $\Theta = (T - T_c)/(T_0 - T_c)$, dimensionless temperature of liquid core; $\pi = P/(P_{max} - P_{min})$, dimensionless pressure in liquid core; $S = c/c_0$, relative impurity concentration; $Fo = Dt/x_0^2$, dimensionless time; $Sm = \nu/D$, Schmidt number; $Le = D/a$, Lewis number; $Gr = \beta[\bar{g}](T_0 - T_c)x_0^3/\nu^2$, thermal Grashof number; $Gr_D = \gamma[\bar{g}]c_0x_0^3/\nu^2$, diffusional Grashof number; h, coordinate-grid step; τ, time-grid step; A, time factor.

LITERATURE CITED

1. P. F. Zavgorodnii, I. L. Povkh, and G. M. Sevast'yanov, Teplofiz. Vys. Temp., 14, No. 4 (1976).
2. Yu. A. Samoilovich, Izv. Akad. Nauk SSSR, Metally, No. 2 (1969).
3. B. I. Vaisman and E. L. Tarunin, in: Hydrodynamics. Scientific Reports of Perm' State University [in Russian], No. 293, Perm' (1972), p. 107.
4. F. V. Nedopekin, Author's Abstract of Candidate's Dissertation, Institute of Hydromechanics, Academy of Sciences of the Ukrainian SSR, Kiev (1976).
5. A. A. Samarskii, Introduction to Difference-Scheme Theory [in Russian], Nauka, Moscow (1971).
6. N. N. Yanenko, Fractional-Step Method of Solving Multidimensional Problems of Mathematical Physics [in Russian], Nauka, Novosibirsk (1967).